Journal of Contaminant Hydrology 235 (2020) 103729

Contents lists available at ScienceDirect

Journal of Contaminant Hydrology

journal homepage: www.elsevier.com/locate/jconhyd

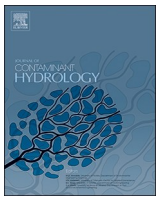

Direct aerobic NSZD of a basalt vadose zone LNAPL source in Hawaii

Thomas McHugh[a,*], Charles Newell[a], Brian Strasert[a], Curtis Stanley[a], Jeff Johnson[b], Thomas Henderson[b], Douglas Roff[c], Joel Narusawa[d]

[a] GSI Environmental Inc., Houston, TX, USA
[b] AECOM, Honolulu, HI, USA
[c] AECOM, San Diego, CA, USA
[d] NAVFAC HI, Honolulu, HI, USA

ARTICLE INFO

Keywords:
Aerobic
Biodegradation
LNAPL
Basalt
NSZD

ABSTRACT

In recent years, a number of methods have been used to measure the biodegradation of petroleum light non-aqueous phase liquids (LNAPL) at petroleum release sites, a process known as natural source zone depletion (NSZD). Most commonly, NSZD rates have been measured at sites with unconsolidated geology and relatively shallow groundwater (< 50 ft. bgs, < 15 m bgs). For this study, we have used two methods (1. carbon dioxide flux measured using carbon traps and 2. heat flux based on subsurface temperature gradients) to measure NSZD rates at a petroleum release site in Hawaii with basalt geology and deep groundwater (> 300 ft. bgs, > 100 m bgs). Both methods documented the occurrence of NSZD at the facility and the two methods yield estimates of the NSZD rate that agreed within a factor of 2 (4600 to 7400 gal/yr; 17,000 to 28,000 L/yr for the flux method and 8600 to 13,000 gal/yr; 33,000 to 49,000 L/yr for the temperature method). Soil gas samples collected directly above the water table and at shallower depths within the vadose zone indicated aerobic conditions throughout the vadose zone (oxygen > 13%) and no detectable methane. These results indicate that NSZD occurs at this site through the direct aerobic biodegradation of LNAPL rather than the two-step process of anaerobic methanogenesis followed by methane oxidation at a shallow depth interval documented at other sites.

1. Introduction

Thousands of sites around the world are affected by historical releases of light non-aqueous phase liquids (LNAPL) such as crude oil, refined fuels, lubricants, and heating oil. Traditionally, active treatment technologies (e.g., hydraulic recovery, air sparging, multi-phase extraction, soil vapor extraction [SVE], etc.) have been applied as common remediation approaches for most LNAPL sites (US EPA, 2005; ITRC, 2009; McHugh et al., 2014). Except for complete excavation, none of these in-situ remediation technologies has been demonstrated to completely remove all the LNAPL within the treatment zone (Sookhak Lari et al., 2020). In recent years, however, there has been an increasing recognition that bacterial degradation of petroleum constituents within LNAPL source areas is an important contributor to LNAPL removal, a process known as natural source zone depletion (NSZD, Garg et al., 2017; Sookhak Lari et al., 2019).

A number of methods have been developed to quantify NSZD rates based on tracking the consumption of oxygen and/or the generation of carbon dioxide (CO_2) associated with biological degradation of petroleum (API, 2017; CRC Care, 2018). These include measurement of CO_2 and oxygen concentration gradients (ITRC, 2009) and the use of dynamic closed chambers (Sihota et al., 2011) and passive CO_2 traps (McCoy et al., 2015) to measure CO_2 flux at the ground surface above LNAPL source areas. All of these methods utilize the measured flux of oxygen into the LNAPL source area or flux of CO_2 out of the LNAPL source area to determine the LNAPL degradation rate (i.e., the amount of LNAPL degradation required to account for the measured amount of oxygen consumption or CO_2 production).

More recently, researchers have developed and demonstrated a temperature-based monitoring method to measure NSZD rates for petroleum LNAPL source areas (Warren and Bekins, 2015; Askarani et al., 2018; Sale et al., 2014). This approach utilizes measurement of the heat generated from biological LNAPL degradation to quantify the LNAPL degradation rate. For this approach i) vertical temperature profiles are collected, recording the soil temperature from ground surface down through the LNAPL source area, ii) this temperature profile is used to determine the heat flux away from the biological reaction zone, and iii) this heat flux is used to calculate the amount of petroleum being degraded (i.e., the volume of petroleum per unit area per unit time required to account for the amount of heat being generated).

* Corresponding author.
E-mail address: temchugh@gsi-net.com (T. McHugh).

https://doi.org/10.1016/j.jconhyd.2020.103729
Received 8 June 2020; Received in revised form 15 September 2020; Accepted 4 October 2020
Available online 06 October 2020

These flux and temperature NSZD measurement methods have shown LNAPL biodegradation rates of 100 s to 1000 s of gallons of LNAPL per acre per year (roughly 1000 s to 10,000 s of kilograms per hectare per year) (Garg et al., 2017) at almost every site where NSZD rates were measured. In addition, these LNAPL removal rates commonly exceed what can be achieved with long-term active LNAPL recovery remedies. As a result, NSZD is gaining broad acceptance as a viable and cost-effective remedy for mature LNAPL releases (Sale et al., 2018a, 2018b). However, to-date, NSZD rates have been reported in the literature at only a few dozen sites in a limited range of environmental settings: typically sites with unconsolidated soils, relatively shallow groundwater (< 50 ft. bgs), and permeable surface cover (i.e., no pavement or buildings). At these sites, NSZD typically occurs as a two-step process: i) anaerobic methanogenic degradation of petroleum constituents within the LNAPL source area and ii) methane oxidation in the vadose zone above the LNAPL source area at the depth interval where upward-diffusing methane meets downward-diffusing oxygen from the ground surface. Because the methane oxidation is the primary heat source for this two-step process, the interval of heat generation corresponds to this methane oxidation zone rather than the depth of the LNAPL source area (Warren and Bekins, 2015). For LNAPLs with a significant volatile fraction, oxidation of VOCs in the vadose zone may also contribute to NSZD (Sookhak Lari et al., 2019).

In this paper, we demonstrate the measurement of NSZD rates for an LNAPL source area at the Red Hill Bulk Fuel Storage Facility (RHBFSF) on Oahu, Hawaii characterized by a high-permeability basalt vadose zone greater than 300 ft. thick. A weathered basalt (saprolite) layer overlies the facility, minimizing recharge from rainfall. To our knowledge, this is one of only a few sites where NSZD rates have been measured in a consolidated (rock) geologic setting and the first example of NSZD that appears attributable to direct aerobic degradation within the LNAPL source area.

2. Methods

The study site consists of 20 very large (12.5 million gallon/47 million L) steel-lined, reinforced concrete (two-and-a-half to four foot thick) underground storage tanks installed within a thick basalt vadose zone such that the base of the tanks is approximately 120 ft. (40 m) above the groundwater table. Each tank is approximately 250-ft (75 m) tall and 100-ft (30 m) in diameter. The tanks have been in service since the mid 1940s, and 18 of the tanks remain in service. The tanks have been utilized primarily for storage of middle-distillate fuels (Jet Fuels, Marine Diesel Fuels) with more limited past storage of gasoline-range fuel. The tanks are arranged in two rows of ten tanks each running from ESE to WNW. A lower access tunnel runs between the two rows of tanks just below the base of the tanks, and an upper access tunnel runs between the two rows of tanks at an elevation of approximately 180 ft. (55 m) above the bottom of the tanks (Fig. 1). In addition to providing access to the tanks for maintenance, the lower access tunnel provides access to 47 soil gas monitoring points (two to three points below each tank), three monitoring wells installed within the tank farm area, and one monitoring well installed downgradient of the tank farm area (Fig. 2). Additional monitoring wells outside the tank farm area used for this study are accessible from ground surface (Fig. 2). Aside from the access tunnels, the native rock around the tanks is largely undisturbed.

The basalt is highly permeable relative to most contaminated sites in unconsolidated settings. The high permeability components of the basalt include massive a'ā (thick/chunky lava flows), clinker zones (layers of gravel-like lava fragments between a'ā layers) described as "*high permeability material analogous to coarse, clean, gravel*" and pāhoehoe (thin/smooth lava flows) that have "*high intrinsic permeability similar to that of carbonate rocks*" (Hunt, 1996). Overall Hunt (1996) reports that when averaged over several lava-flow thicknesses, the lateral hydraulic conductivity of dike free lava flows such as found in the vicinity of Red Hill is about 500 to 5000 ft per day (0.18 to 1.8 cm/s). This is about 23 to 230 times higher than the median hydraulic conductivity of 0.008 cm/s for 191 contaminated sand and gravel groundwater sites from Newell et al. (1990). Due to this high permeability, advective or diffusive air penetration into the unsaturated basalt is much more likely than for sites comprised of unconsolidated media.

Prior investigation results indicate historical petroleum fuel releases prior to 1988 of unknown volume from several tanks and one more recent release of 27,000 gal (100,000*L*) of jet fuel in 2014. Evidence of prior releases includes visible staining and detection of Total Petroleum Hydrocarbons (TPH) in rock cores collected from angled borings completed below the fuel tanks in the late 1990s and early 2000s documenting the presence of LNAPL within a depth interval of approximately 10 ft. to 30 ft. (3 to 10 m) below the bottom of the fuel tanks. These angled borings were later converted to soil gas monitoring points (Fig. 1). LNAPL has not been observed in groundwater (approximately 120 ft., 35 m below the bottom of the fuel tanks) in any of the monitoring wells.

The RHBFSF has implemented modern release prevention and release detection technologies. The purpose of this study was to better understand NSZD rates and processes for historical releases.

Three methods were applied to quantify NSZD rates for LNAPL associated with these prior releases: i) the passive CO_2 trap method with traps installed at the surface of the facility; ii) an adapted CO_2 trap method where CO_2 was measured in the exhaust from the ventilated Red Hill tunnel system; and iii) the temperature method. In addition, oxygen, CO_2, and methane concentrations and differential pressure were measured at each below-tank soil gas point and monitoring well headspace.

2.1. Carbon trap measurements

Carbon traps from *E*-Flux (Fort Collins, CO) were used to measure the flux of CO_2 at the ground surface and through the two access tunnels. Flux at the ground surface was measured by deploying eight standard E-Flux carbon traps; two transect lines of four traps were deployed, each transverse to the rows of tanks resulting in two carbon traps north of the tanks, four traps above the tanks, and two traps south of the tanks. The surface traps were deployed for 14 days in the fall of 2017 (Fig. 3).

CO_2 flux within the two tunnels was measured using custom packed carbon trap cartridges from *E*-Flux. These cartridges were deployed at three locations: i) an air intake point for the tunnel system, ii) the air exhaust point for the upper tunnel, and iii) the air exhaust point for the lower tunnel. At each location, two consecutive 24 h samples were collected in the fall of 2017 by pumping air through the carbon traps at a constant pumping rate of 1.06 L/min. A mass flow controller was used to maintain a constant air pumping rate.

The carbon trap samples were analyzed by E-Flux to measure the mass of CO_2 on each trap. ^{14}C measurements were used to apportion the mass of CO_2 in each sample between modern sources and fossil fuel sources (Hua et al., 2013; McCoy et al., 2015). For the aboveground traps, the mass of fossil fuel-associated CO_2 was converted into a carbon flux by E-Flux (E-Flux, 2014). For the tunnel carbon trap cartridges, the CO_2 mass was converted into a concentration in tunnel air using the known sample volume. This concentration was converted into a flux by multiplying the concentration by the forced air ventilation rate for the tunnel. The CO_2 flux rate was used to calculate a fuel degradation rate using the stoichiometry of fuel degradation: 1 mol $C_{11}H_{24}$ yields 11 mol CO_2.

2.2. Temperature measurements

Vertical temperature profiles were collected October 2017 and April 2019. During both events, temperature profiles were measured at the four monitoring wells accessed from the lower access tunnel. One outside well was measured in October 2017 and seven outside wells

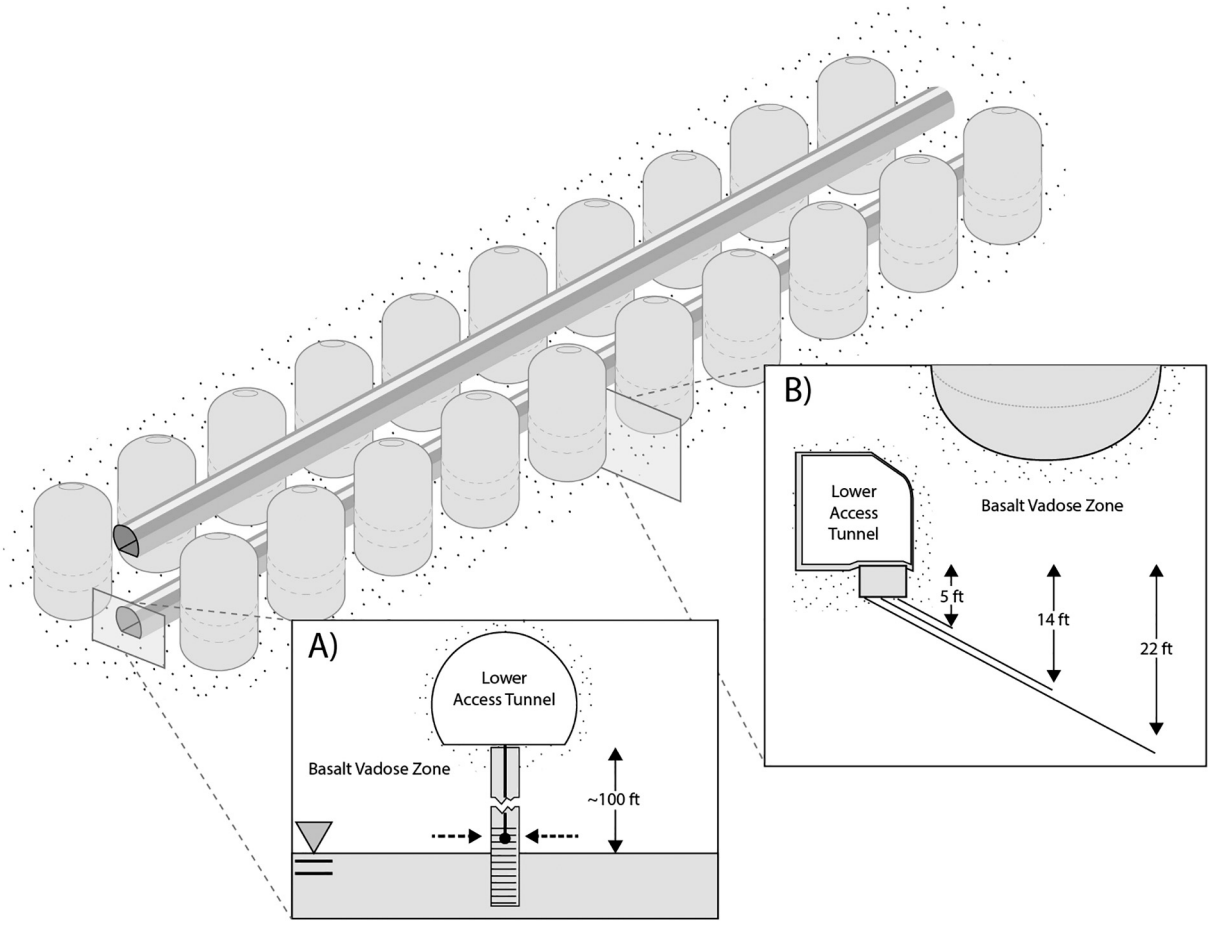

Fig. 1. Design of soil gas sample points accessible from Lower Access Tunnel. (A) Monitoring wells screened partly above the water table. (B) Soil gas monitoring points installed below each active tank. Distances shown are depths below the floor of the lower tunnel.

were measured in April 2019. Temperature measurements were obtained using a high accuracy Type-T thermocouple (Physitemp Instruments). During the October 2017 event, well air temperatures were measured two ways: 1) by allowing the thermocouple to hang vertically at each measurement depth in air within the well; and 2) by pressing the thermocouple against the sidewall using a pipe test-ball plug to obtain well sidewall temperatures. At each depth, the thermocouple reading typically stabilized within 2–3 min. The two temperature measurement techniques provided similar results. In April 2019, only well air temperatures (method 1) were measured because the two measurement methods yielded comparable results in October 2017. In October 2017, temperature measurements were collected at five-foot

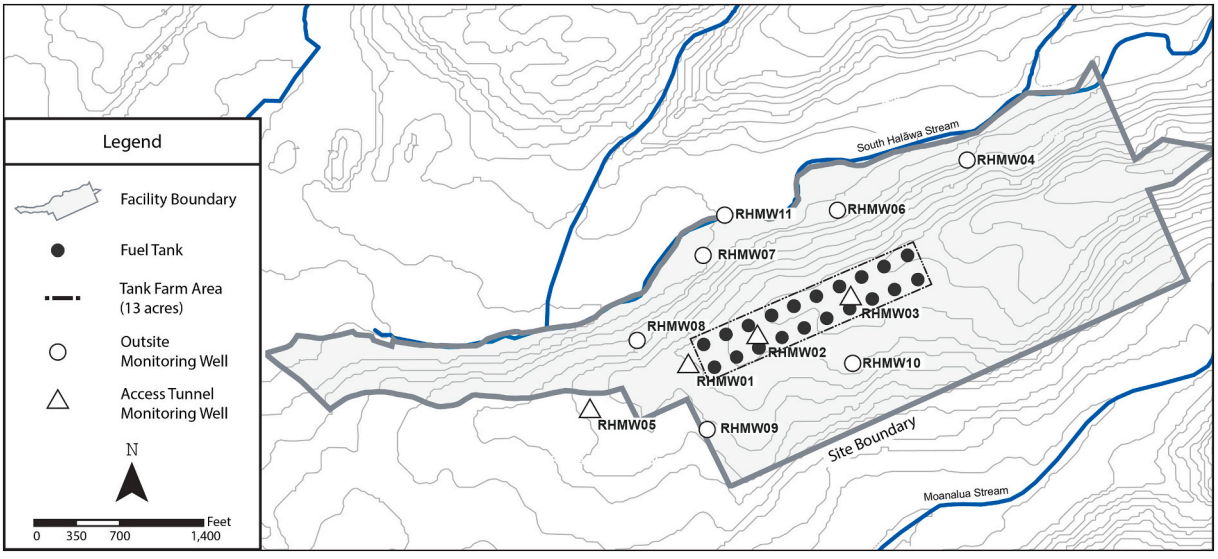

Fig. 2. Monitoring well locations used for this study.

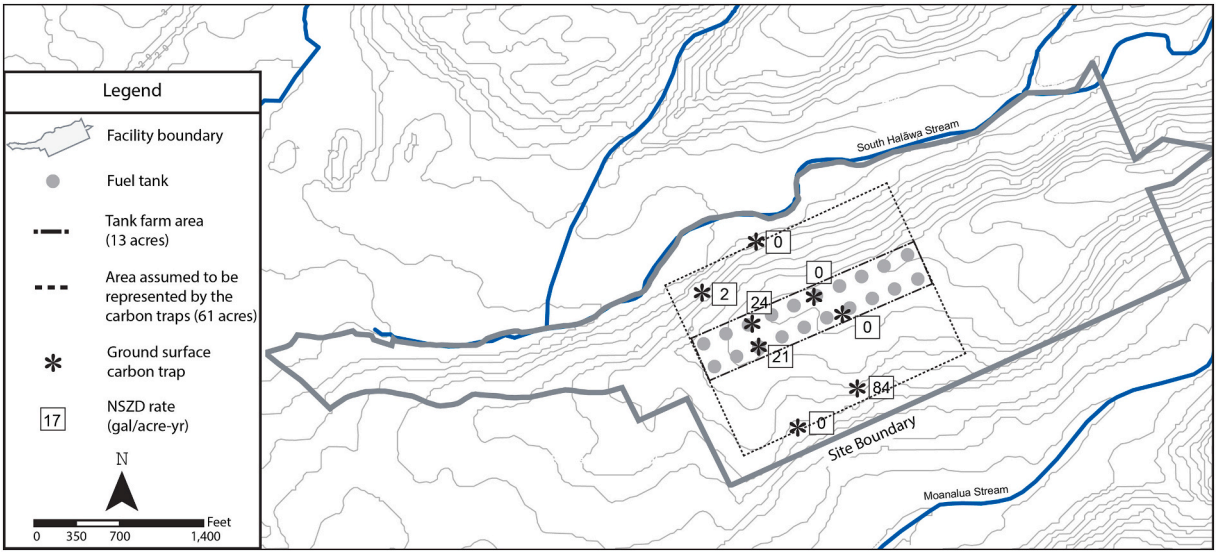

Fig. 3. Ground surface carbon trap locations and results.

(1.5 m) depth intervals from the ground surface to the bottom of each well. In April 2019, variable depth intervals were used ranging from 1 ft. to 20 ft. (0.3 to 6 m).

2.3. Methane, oxygen, CO_2, and differential pressure

Methane, oxygen, CO_2, and differential pressure were measured in September 2017 at the soil gas monitoring points underlying the Facility tanks and at in-tunnel monitoring wells with screens partially above the water table (i.e., RHMW02, RHMW03, and RHMW05). The monitoring wells were sealed with a gas-tight cap at least 24 h before sample collection. At each sample point, a syringe pump was used to pump 750 mL of headspace vapor into a Tedlar bag. For these monitoring locations, the sample was collected using a weighted 1/8 in. (3 mm) nylon tube threaded through the gas-tight cap and lowered into the well to a depth of two feet above the water table so that the sample was collected within the uncased well interval, immediately above the water table. A GEM5000 Landfill Gas Meter was used to measure oxygen, CO_2, and methane concentrations in the bag. The meter reading typically stabilized after approximately 1 min (i.e., 500 mL based on a pumping rate for the landfill gas meter of approximately 500 mL/min), and the reading was recorded when the bag was almost emptied by the meter. A charcoal filter cartridge was installed in the sample line between the water filter and the Tedlar bag to prevent false positive methane readings associated with petroleum vapors in the samples. The charcoal filter removes larger petroleum VOCs, but does not remove methane (Jewell and Wilson, 2011). Following completion of the fixed gas readings, differential pressure was measured by connecting the GEM5000 directly to the soil vapor well or monitoring well.

For all of the monitoring well headspace sample locations and 18 of the below-tank soil gas points, samples were also collected using a 2.7 L Summa canister for analysis of oxygen, CO_2, methane, and nitrogen by EPA Method 3C by Alpha Analytical Laboratory, Westborough, MA. Samples were analyzed for an expanded list of 90 petroleum VOCs by EPA Method TO-15. Total petroleum VOC concentrations were low (6 to 300 ppbv; median = 20 ppb) in all samples and are not discussed further.

3. Results

3.1. Methane, oxygen, CO_2

High oxygen and low CO_2 concentrations were recorded at almost all measurement locations. In the 47 below-tank soil vapor points, oxygen concentrations ranged from 13.7% to 20.6%, with only two readings below 18%. CO_2 concentrations ranged from 0.1% to 3.2%, with most readings less than 1%. For the well headspace samples, oxygen was 6.6–21% and CO_2 was 0.1–8.5%. Methane was never detected in any measurement location using either the landfill gas meter (detection limit = 0.1%) or samples analyzed off-site by EPA Method 3C (detection limit = 0.06%). These results show an aerobic environment throughout the vadose zone. The lowest oxygen concentrations were measured in the headspaces of RHMW02 (6.6%) and RHMW03 (17%), locations where the temperature measurements indicated the occurrence of NSZD. The results for the individual sample points are provided as supplemental materials, Table S.1.

3.2. Differential pressure

For 39 of the 46 below-tank soil vapor wells tested and three of four monitoring wells, the differential pressure measurements showed a negative pressure in the tunnel relative to the basalt (i.e., a pressure gradient indicating gas flow from the vadose zone into the tunnel). At most of these locations, the differential pressure was greater than 0.1 in. H_2O (i.e., > 25 Pa). For comparison, a differential pressure of 0.02 in. H_2O (5 Pa) is typically considered sufficient to support advective flow for vapor intrusion mitigation (i.e., sufficient for effective sub-slab depressurization systems). These results indicate that tunnel exhaust system maintains a negative air pressure that supports advective air flow from the vadose zone into the tunnels, mimicking the effects of a soil vapor extraction system.

3.3. Carbon trap results

Eight passive CO_2 traps were used to measure the flux of fossil fuel-associated CO_2 to the ground surface. No fossil fuel CO_2 was detected on four of the traps (< 0.001 g). For the remaining four traps, over the 14-day deployment time, the mass of fossil fuel CO_2 accumulated on each trap ranged from 0.002 g to 0.06 g, corresponding to equivalent NSZD rates of 2 to 84 gal/acre/yr (19 to 784 kg/ha/yr) (Fig. 3). The average NSZD rate across the eight traps was 16 +/− 29 gal/acre-yr (149 +/− 271 kg/ha/yr). The variability in NSZD rates between traps was not unexpected due to i) the large vertical distance of greater than 300 ft. between the likely NSZD reaction zone and ground surface, and ii) the heterogenous spatial nature of CO_2 flux to the surface that can cause orders of magnitude differences in spatial samples (e.g., Garg

Table 1
Tunnel system carbon cartridge results.

Sample	Fossil fuel CO_2 (g)
Lower tunnel air exhaust day 1	0.081
Lower tunnel air exhaust day 2	0.085
Upper tunnel air exhaust day 1	0.022
Upper tunnel air exhaust day 2	0.037
Tunnel air intake day 1	0.033
Tunnel air intake day 2	−0.006

Table 2
NSZD rates attributable to flux of fossil fuel CO_2.

Flux pathway	Lower bound rate (Gallons/Year)	Upper bound rate (Gallons/Year)
Upper tunnel exhaust	200	530
Lower tunnel exhaust	3400	5900
Ground surface (Best Estimate)		980
TOTAL SITEWIDE NSZD RATE	4600	7400

et al., 2017). A layer of variable thickness lower-permeability saprolite at ground surface directly above the tanks and exposed basalt layers north and south of the tanks may affect the area where CO_2 from NSZD is expressed at ground surface. An estimate of overall NSZD attributable to the flux of CO_2 to ground surface was calculated by multiplying the average NSZD rate from the eight traps (16 gal/acre-yr) by the ground surface area at the facility within the carbon trap deployment area (61 acres) yielding a site-wide NSZD rate of 980 gal/year. Note that the 61 acre ground surface area includes the approximately 13 acre area of the tank farm plus additional land area to the north and south included within the carbon trap test area to evaluate lateral migration of CO_2 within the subsurface (Fig. 3).

In the second carbon trap method, six carbon cartridges were used to trap CO_2 from a known volume of air (1401 L to 1540 L) from the tunnel system that provides access to the fuel storage tanks. Following a 24 h sample period, the mass of fossil fuel CO_2 accumulated on each trap ranged from −0.006 g to +0.085 g (Table 1). The small negative value for one of the samples at the tunnel air intake point reflects analytical variability and uncertainly associated with use of ^{14}C composition to distinguish between modern CO_2 and fossil fuel CO_2.

The detection of excess fossil fuel CO_2 at tunnel air intake was not expected because the ^{14}C correction accounts for the typical composition of CO_2 in atmospheric air (E-Flux, 2014). However, during sample collection, a large diesel generator was operating outdoors approximately 50 ft. from the air intake where the intake air sample was collected. The generator may have been a source of the excess fossil fuel CO_2 in the intake air sample collected on Day 1 (Table 1). For safety reasons, no combustion engines or other fossil fuel combustion sources are allowed within the tunnel system. As a result, the increase in fossil fuel CO_2 between the tunnel air intake and the tunnel air exhaust points indicates capture of CO_2 from the biodegradation of LNAPL sources areas within the basalt.

The tunnel system has two primary air intakes; the second air intake is located several hundred feet from any combustion sources. Because testing was conducted at only one of the air intake points, there was some uncertainty regarding the average concentration of excess fossil fuel CO_2 in the air being taken into the tunnel system during the testing program. To address this uncertainty, upper and lower bound NSZD rates were calculated for NSZD attributable to fossil fuel CO_2 at the tunnel air exhaust points. The upper bound NSZD rates were calculated assuming that 100% of the fossil fuel CO_2 at the tunnel exhaust points was attributable to biodegradation of LNAPL. The lower bound NSZD rates were calculated based on the difference in fossil fuel CO_2 between the measured tunnel air intake and the tunnel air exhaust.

Combining the NSZD attributable to the flux of fossil fuel CO_2 to the ground surface with the NSZD attributable to the flux of fossil fuel CO_2 into the access tunnel system yields an overall NSZD rate at the facility of 4600 to 7400 gal/year (17,000 to 28,000 L/yr; Table 2). Assuming a tank farm area of 13 acres, this corresponds to a NSZD rate of 350 to 570 gal per acre per year (3200 to 5300 kg/ha/yr). Note that an area of 61 acres was used to calculate the CO_2 flux at ground surface, corresponding to the surface area covered by the network of ground surface carbon traps. However, a smaller area of 13 acres was used to estimate the overall NSZD rate per unit area. 13 acres corresponds to the area containing the 20 fuel tanks (Fig. 3). This is the maximum area impacted by fuel releases from the facility assuming that lateral migration of LNAPL has been minimal. The assumed LNAPL-impacted area affects NSZD rate per unit area but does not affect the total NSZD rate for the facility estimated from the flux of fossil fuel CO_2.

3.4. Temperature results

Most applications of the temperature method for quantifying NSZD rates have utilized in-place thermocouples to record daily vertical temperature profiles over a period of months or longer in the vadose zone at locations within and outside the petroleum impacted area (Warren and Bekins, 2015; Askarani et al., 2018). Long-term installation of temperature profiling equipment was determined not to be feasible at this facility. However, Sweeney and Ririe (2014) indicate that “snap shot” temperature profiles provide a reliable way to understand in-situ biodegradation. At this site, the thick vadose zone (≅120 ft. from the base of the fuel tanks to the water table) was expected to yield a more stable vertical temperature profile compared to sites with shallow groundwater, increasing the reliability of the snap shot approach.

Subsurface temperatures were measured during two field events: October 2017 and April 2019 (supplemental materials Table S.2 and S.3). The first event included four monitoring wells installed inside the lower access tunnel and one well installed outside the tunnel system. The second field program included these five wells plus six additional wells installed outside the tunnel system. For each well, temperatures were measured at 16 to 61 depth intervals from the surface to the bottom of the well, generally 10 ft. to 20 ft. (3 to 6 m) below the water table. During the October 2017 event, measurements of well air temperature and well wall temperature yielded similar results (Fig. 4). Based on this finding, only well air temperatures were measured during the April 2019 event. For consistency between the two events, the well air temperature data have been used for the evaluation of NSZD rates.

The seven monitoring wells (used in this study) outside of the lower access tunnel are located north or south of the tank farm area (Fig. 2). These wells exhibited relatively consistent vertical temperature profiles with temperatures near ground surface that were close to the mean annual air temperature at the Honolulu International Airport 25.4 °C (1981–2010; National Oceanic and Atmospheric Administration (NOAA), 2020). For these wells, temperature decreased with depth down to the groundwater reaching a temperature of 21.0 °C to 22.5 °C, consistent with background groundwater temperatures in the area (supplemental materials Table S.3). None of these wells exhibited an increase in temperature within the depth interval between the base of the fuel tanks and the water table, suggesting an absence of subsurface heating associated with biodegradation of LNAPL.

The four wells located inside the lower access tunnel showed very consistent temperature profiles between the October 2017 and April 2019 field events particularly at depths of more than 15 ft. below the top of the well. Although the lower tunnel is located more than 350 ft. (110 m) below ground surface, the use of ambient air for tunnel ventilation is expected to cause some seasonal variation in tunnel temperature that could impact vadose zone temperatures within a few feet of the tunnel.

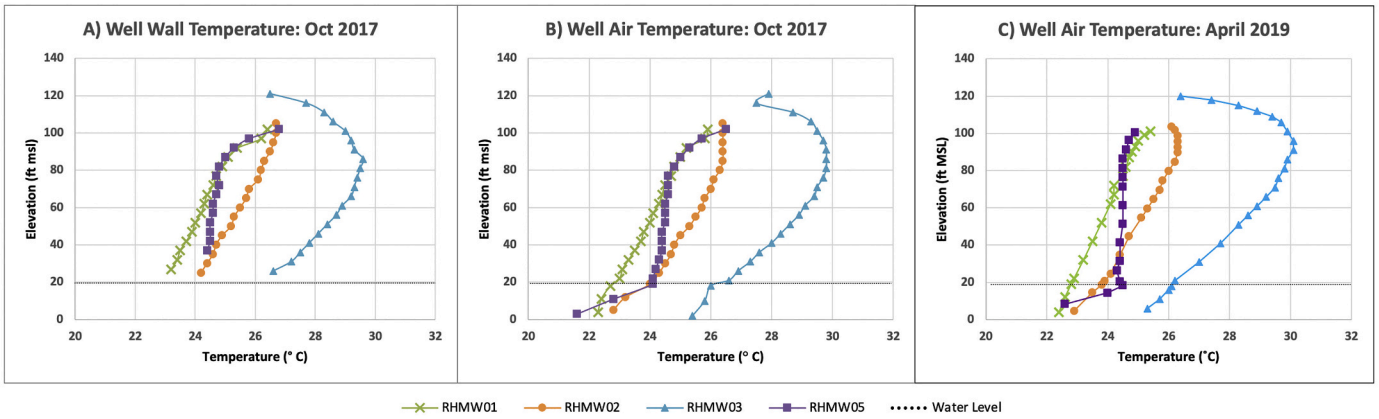

Fig. 4. Vertical temperature profiles for tunnel monitoring wells.

For the purpose of determining NSZD rates, vertical temperature profiles are used to determine the upward temperature gradient (from heat source to the lower tunnel) and downward temperature gradients (from heat source to groundwater) from the aerobic NSZD reaction zone between the lower tunnel and groundwater. These temperature gradients were used to determine temperature-based NSZD rates as described in Sweeney and Ririe (2014), Warren and Bekins (2015), and Sale et al., 2014; Sale et al., 2018b. Determining the upward temperature gradient attributable to subsurface heating typically requires a background location to correct for the effect of seasonal temperature variations on shallow vadose zone temperatures (Askarani et al., 2018).

Two tunnel wells located within the tank farm (RHMW02 and RHWM03) exhibited temperatures profiles consistent with a subsurface heat source below the lower tunnel within the depth interval of 80 ft. to 100 ft. (24 to 30 m) above mean sea level (msl). Because all the site soil gas and high-permeability geology indicates that NSZD-related biodegradation at this site is aerobic, the temperature profiles provide reliable information about the vertical interval of LNAPL in the vadose zone in the vicinity of the monitoring wells. At these two locations, the groundwater temperature at the top of the water table (23.8 °C and 26.0 °C) was well above the background range of 21.0 °C to 22.5 °C, and the groundwater temperature decreased with depth below the water table, two factors consistent with a substantial vadose zone heat source. The other two tunnel wells (RHMW01 and RHMW05) are located between the tank farm area and a large pumping well that likely controls the flow of groundwater within the area. Assuming groundwater flow from the tank farm to the pumping well, RHMW01 is located at the downgradient edge of the tank farm and RHMW05 is located approximately halfway between the edge of the tank farm and the pumping well. These two wells exhibited elevated groundwater temperatures at the top of the water table (22.8 °C and 24.5 °C), but vadose zone temperature profiles were less indicative of vadose zone heating, suggesting that these two wells are both located downgradient of the primary NSZD heat generation area. While the temperature profile for RHMW05 shows no evidence of vadose zone heating, the temperature profile for RHMW01 show a small inflection at depth of approximately 25 ft. below the lower tunnel floor that could be indicative of a small amount of heat generation (see Supplemental Materials).

Because the temperature profile for RHMW01 was potentially consistent with either background temperature conditions or with a small amount of vadose zone heat generation, two set of NSZD rates were calculated: i) NSZD rates were calculated for three locations (RHMW01, RHMW02, and RHMW03) using RHMW05 for background correction and ii) NSZD rates were calculated for two locations (RHMW02, and RHMW03) using RHMW01 for background correction. The NSZD calculations are provided as supplemental materials and the results are summarized in Table 3.

Averaging across the three wells located within the tank farm area and using a tank farm area of 13 acres, the temperature data indicate an overall NSZD rate for the facility of 8600 gal/year to 13,000 gal/year (33,000 to 49,000 L/yr), within a factor of two of the rate range estimated based on the CO_2 flux.

Table 3
NSZD Rates from Temperature Profiles in Monitoring Wells Extending from Lower Access Tunnel to Groundwater.

	RHWM01	RHMW02	RHMW03
Upward Heat Flux (W/m^2)	0–0.07	0.52–0.67	1.59–1.92
Downward Heat Flux (W/m^2)	0–0.15	0.02–0.17	0.10–0.31
NSZD Rate (gal/acre-year)	0–200	490–750	1500–2000
TOTAL SITEWIDE NSZD RATE (gallons per year)	8600 to 13,000		

4. Discussion

Two different methods (CO_2 flux and heat flux) were used to measure the rate of NSZD at a large petroleum storage facility in Hawaii. Both fossil fuel-associated CO_2 and excess heat were measured at the facility providing strong evidence that NSZD is occurring. The estimated petroleum degradation rates were 4600 to 7400 gal/year (17,000 to 28,000 L/yr) based on CO_2 flux and 8600 to 13,000 gal/year (33,000 to 49,000 L/yr) based on heat flux. The relatively close agreement in NSZD rates between the two methods provides increased confidence in the overall findings. In addition, the monitoring wells adjacent to the tanks and screened below likely zones of LNAPL within the vadose zone showed groundwater temperatures were elevated by 3 °C to 5 °C relative to monitoring wells not located in the immediate vicinity of the tanks (data not shown), confirming the presence of a large biodegradation-related heat source in the vadose zone. Note that the datasets for the two evaluation methods (CO_2 flux and heat flux) do not support an evaluation of spatial consistency (i.e., whether or not the two methods indicate that NSZD is occurring in the same area).

Oxygen, CO_2, and methane concentrations were measured in vadose zone samples collected from available soil gas monitoring points installed below the fuel tanks and well headspace samples for monitoring wells screened across the water table. These samples showed no detectable methane (< 0.1%) in any samples and oxygen concentrations indicative of aerobic conditions throughout the vadose zone. These results indicate that the common NSZD two-step process of anaerobic methanogenic degradation of petroleum constituents within the LNAPL source area and methane oxidation at a shallower depth interval in the vadose zone (e.g., Garg et al., 2017; Warren and Bekins, 2015) is not applicable at this site. Instead, the occurrence of high oxygen concentrations throughout the vadose zone suggest that NSZD is occurring

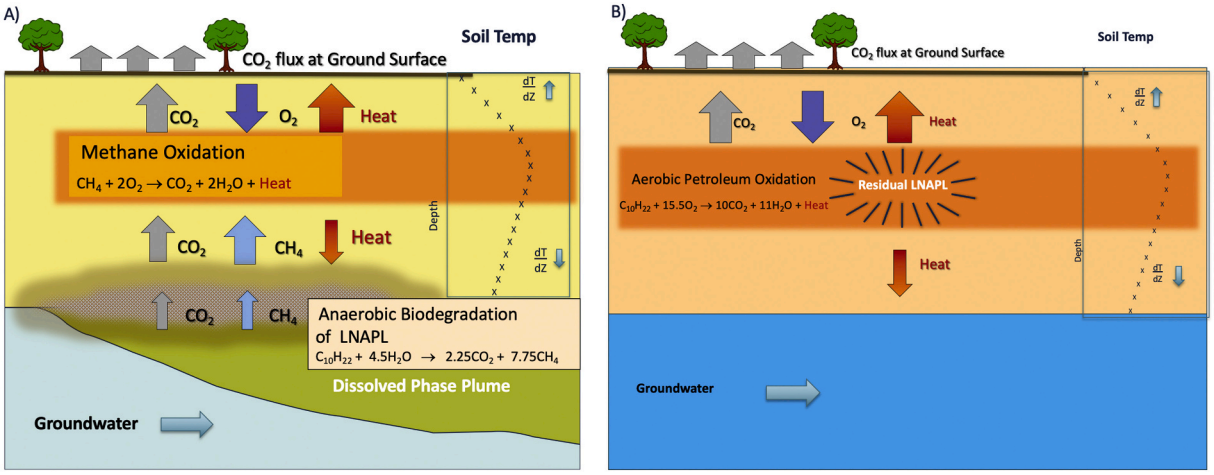

Fig. 5. Conceptual model of A) conventional two-stage NSZD in unconsolidated media and B) NSZD through direct aerobic biodegradation of LNAPL in high permeability media such as basalt. The available soil gas and geologic data support an aerobic NSZD Conceptual Site Model at the Red Hill Facility. (For interpretation of the references to colour in this figure legend, the reader is referred to the web version of this article.)

through the direct aerobic degradation of LNAPL within the vadose zone (Fig. 5) and that the elevated temperature in the vertical temperature profiles at two of the monitoring wells correspond to the location of LNAPL that is being biodegraded aerobically.

Although no methane was detected above or below the LNAPL source, no methane or oxygen measurements were taken directly within the LNAPL source area. Thus, it is possible that the LNAPL source area may contain an anaerobic methanogenic core with methane oxidation occurring above and below this anaerobic core.

The differential pressure measurements indicate that the pressure within the lower tunnel is lower than the pressure in the surrounding basalt, supporting the flow of air from the basalt into the tunnel. In addition, the measurement of fossil fuel-associated CO_2 in the lower tunnel is consistent with air flow from the LNAPL source area into the lower tunnel. Together, these results indicate that the low pressure in the lower tunnel is acting as a very large vapor extraction system inducing air flow through the vadose zone into the lower tunnel. This induced air flow may contribute to the maintenance of aerobic conditions within the LNAPL source area. To our knowledge, this is the first petroleum release site where the available data support a conceptual model of direct aerobic biodegradation of LNAPL in the vadose zone and provides NSZD rates of LNAPL in a basalt vadose zone.

Declaration of Competing Interest

None.

Acknowledgements

The field work and data evaluation for this research was funded by the U.S. Navy under Comprehensive Long-term Environmental Action *Navy* (CLEAN) Contract No. N62742-17-D-1800. Development of the manuscript was funded by GSI Environmental Inc. Project 9400905. The authors thank Poonam Kulkarni of GSI Environmental and staff from the Navy, AECOM, and GSI Environmental for assistance in planning and implementation the field study. The authors also thank Barbara Bekins of the United States Geological Service for helpful input on interpretation of the temperature data.

Appendix A. Supplementary data

Supplementary data to this article can be found online at https://doi.org/10.1016/j.jconhyd.2020.103729.

References

American Petroleum Institute, 2017. Quantification of Vapor Phase-related Natural Source Zone Depletion Processes. (Publication 4784).

Askarani, K.K., Stockwell, E.B., Piontek, K.R., Sale, T.C., 2018. Thermal monitoring of natural source zone depletion. Groundwater Monitor. Remed. 38 (3), 43–52. https://doi.org/10.1111/gwmr.12286.

CRC CARE, 2018. Technical measurement guidance for LNAPL natural source zone depletion. In: CRC CARE Technical Report no. 44, CRC for Contamination Assessment and Remediation of the Environment, Newcastle, Australia.

E-Flux, 2014. Differentiating Petroleum Hydrocarbon and Modern Carbon Using CO_2 Flux Traps. E-Flux, Ft Collins, Colorado (June 03, 2014).

Garg, S., Newell, C., Kulkarni, P., King, D., Irianni Renno, M., Sale, T., 2017. Overview of natural source zone depletion: processes, controlling factors, and composition change. Groundwater Monitor. Remed. 37 (3), 62–81. https://doi.org/10.1111/gwmr.12219.

Hua, Q., Barbetti, M., Rakowski, A.Z., 2013. Atmospheric radiocarbon for the period 1950–2010. Radiocarbon 55 (4), 2059–2072.

Hunt, C.D., 1996. Geohydrology of the Island of Oahu, Hawaii. U.S. Geological Survey Professional Paper 1412-B.

ITRC, 2009. Evaluating LNAPL Remedial Technologies for Achieving Project Goals. Interstate Regulatory and Technology Council, Technical/Regulatory Guidance, December 2009.

Jewell, K.P., Wilson, J.P., 2011. A new screening method for methane in soil gas using existing groundwater monitoring Wells. Groundwater Monitor. Remed. 31 (3), 82–94.

McCoy, K., Zimbron, J., Sale, T., Lyverse, M., 2015. Measurement of natural losses of LNAPL using CO_2 traps. Groundwater 53, 658–667. https://doi.org/10.1111/gwat.12240. Available at: http://onlinelibrary.wiley.com/doi/10.1111/gwat.12240/abstract.

McHugh, T.E., Kulkarni, P.R., Newell, C.J., Connor, J.A., Garg, S., 2014. Progress in remediation of groundwater at petroleum sites in California. Groundwater 52 (6), 898–907. https://doi.org/10.1111/gwat.12136.

National Oceanic and Atmospheric Administration (NOAA), 2020. Climate Data Online. Available at. https://www.ncdc.noaa.gov/cdo-web/ (Accessed January 6, 2020).

Newell, C.J., Hopkins, L.P., Bedient, P.B., 1990. A hydrogeologic database for groundwater modeling. Ground Water 28 (5).

Sale, T., E. Stockwell, C. Newell, and P. Kulkarni, 2014. Subsurface Thermal Flux Tools, Provisional US Patent No. 61/941,194, Feb. 18, 2014.

Sale, T., Hopkins, H., Kirkman, A., 2018a. Managing Risks at LNAPL Sites. 2nd Edition Bulletin 18. American Petroleum Institute.

Sale. T., E. B. Stockwell, C. J. Newell, and P.R. Kulkarni, 2018b. Devices and Methods for Measuring Thermal Flux and Estimating Rate of Change of Reactive Material Within a Subsurface Formation. US Patent 10,094,719 B2. Oct. 9, 2018.

Sihota, N.J., Singurindy, O., Mayer, K.U., 2011. CO2-efflux measurements for evaluating source zone natural attenuation rates in a petroleum hydrocarbon contaminated aquifer. Environ. Sci. Technol. 45 (2), 482–488. https://doi.org/10.1021/es1032585. Available at: http://pubs.acs.org/doi/abs/10.1021/es1032585.

Sookhak Lari, K., Davis, G.B., Rayner, J.L., Barstow, P.B., Puzon, G.J., 2019. Natural source zone depletion of LNAPL: a critical review supporting modelling approaches. Water Res. 157 (2019), 630–646. https://doi.org/10.1016/j.watres.2019.04.001.

Sookhak Lari, K., Rayner, J.L., Davis, G.B., Johnston, C.D., 2020. LNAPL recovery endpoints: lessons learnt through modeling, experiments, and field trials. Groundwater Monitor. Remed. https://doi.org/10.1111/gwmr.12400. In Press.

Sweeney, R.E., Ririe, G.T., 2014. Temperature as a tool to evaluate aerobic biodegradation in hydrocarbon contaminated soil. Groundwater Monitor. Remed. 34, 41–50.

U.S. EPA, 2005. A Decision-Making Framework for Cleanup of Sites Impacted with Light Non-Aqueous Phase Liquids (LNAPL). EPA 542-R-04-01. March 2005.

Warren, E., Bekins, B.A., 2015. Relating subsurface temperature changes to microbial activity at a crude oil-contaminated site. J. Contam. Hydrol. 182 (2015), 182–193. https://doi.org/10.1016/j.jconhyd.2015.09.007.